J Mater Sci (2007) 42:40–49
DOI 10.1007/s10853-006-1038-z

Low-cycle fatigue behavior of AISI 347 stainless steel in salt water

Chih-Kuang Lin · Chui-Hsien Chiu

Received: 15 September 2005 / Accepted: 18 January 2006 / Published online: 15 November 2006

Abstract The aim of this study is to investigate the influence of strain ratio, frequency, and waveform on low cycle fatigue (LCF) behavior of AISI 347 stainless steel in air and NaCl solution. Results showed that at high strain amplitude region the fatigue lives in both environments were comparable, implying a lack of environmental effect due to insufficient amount of local dissolution. However, at low strain amplitude region, a corrosive effect did exist and the fatigue lives in NaCl solution were decreased with an increase in strain ratio to a greater extent, as compared to those in air. This might be attributed to a tensile-mean-stress effect and its interaction with an enhanced, localized corrosive reaction. The degree of influence of the aggressive salt water on the LCF life was not increased as the loading frequency was reduced or a hold time was added at the tensile peak strain. The LCF life data in the given environments at various strain ratios could be well correlated by a modified SWT model as well as a modified Manson-Halford model.

Introduction

AISI 347 stainless steel (SS) was developed to improve the resistance of 304 austenitic SS to intergranular stress corrosion cracking (IGSCC) by adding niobium (Nb) to form niobium carbides in preference to Cr-rich carbides so that the depletion of chromium at grain boundary regions could be reduced [1]. Most of the previous studies on AISI 347 SS were focused on microstructure analysis [2, 3], corrosion properties [4, 5], sensitized degradation [6, 7], hydrogen embrittlement [8–11], creep [12–14], and high-temperature brittle fracture [15, 16]. As some applications of this austenitic SS, e.g. in conventional and nuclear power plants, are often subjected to cyclic stresses in aggressive environments, corrosion fatigue (CF) properties are essentially needed in the safe life design of components made from this alloy. However, little work has been done on the fatigue strength [17] and there is still lack of systematic studies on the CF properties for this alloy. A series of studies on the CF properties of AISI 347 SS were thus planned and conducted by the authors so as to better assess and predict the service life of the components made of this alloy used in corrosive environments. Investigation of the environmental effects on the high-cycle fatigue (HCF) and fatigue crack growth (FCG) for this alloy has been completed in an earlier work [18].

Many of the engineering components contain notches or other types of geometric discontinuities. The stress concentration effects from these geometric discontinuities would generate localized, extensive plastic deformation. If such components are subjected to cyclic loading in corrosive environments, low-cycle corrosion fatigue (LCCF) will take place at the regions around the notch roots. As part of a series of studies on the CF properties of AISI 347 SS [18], the objective of the present study is to characterize the low-cycle fatigue (LCF) behavior of such material in air and salt water. In this study, systematic experiments were conducted to investigate the influence of strain rate, mean stress, and tensile hold time on the LCCF

C.-K. Lin (✉) · C.-H. Chiu
Department of Mechanical Engineering, National Central University, Chung-Li 32054, Taiwan
e-mail: t330014@cc.ncu.edu.tw

behavior of 347 SS in salt water with comparison to that in air.

Experimental procedures

The commercially available AISI 347 SS used in the current study was supplied by the vendor in the form of solution-annealed round bars. The chemical composition of this alloy (wt%) is 17.28 Cr, 10.23 Ni, 1.67 Mn, 0.63 Nb, 0.59 Si, 0.09 Mo, 0.08 Cu, 0.05 Co, 0.05 C, 0.035 N, 0.025 S, 0.023 P, <0.01 Ta and Fe (balance). Axial smooth-surface specimens with a uniform cylindrical gage section of 6 mm in diameter and 24 mm in length were used for LCF testing. The specimens were heat-treated at 1050°C for 1 h and then water quenched to obtain a solution-annealed condition of which the mechanical properties have an ultimate tensile strength of 658 MPa, a yield strength of 310 MPa, an elastic modulus of 190 GPa, an elongation of 61.4% (in 25 mm), and a hardness value of 42 HRb.

In this study, LCF tests were conducted in air and 3.5% NaCl (pH = 5.75) solution. A special acrylic cell was fabricated for LCF testing in the aqueous environment. The cell enclosed the gage section of the specimen in a fully submerged condition during fatigue testing as shown in Fig. 1. A circulated loop was made by pumping the corrosive solution back to an external reservoir located at higher place and making it flow through the acrylic cell to another lower tank. The LCF tests were carried out under total axial strain control on a commercial closed-loop servo-hydraulic test machine. To avoid the interference with the acrylic cell, a modified, extended extensometer with a gage length of 20 mm was used to perform the strain-control function. A set of LCF tests with several applied strain amplitudes ranging from 0.3 to 0.7% were performed under an 1-Hz triangular waveform at strain ratios of $R = -1$, 0, 0.5, and 0.8 in air and salt water. To explore the strain rate effects, a second set of LCF tests under a 0.1-Hz triangular waveform were conducted at a strain ratio of 0.5 with a strain amplitudes of 0.3% in the aforementioned environments. To investigate the hold-time effect, a hold period of 10 s added at the tensile peak strain in a pure 1-Hz triangular waveform (ramping portion), i.e. to become a trapezoidal waveform, was applied to perform the third set of LCCF tests at a strain ratio of 0.5 with an amplitude of 0.3% in the salt water. A 50% drop of the peak load was defined as specimen failure. Characterizations of the fracture surface morphology were made by scanning electron microscopy (SEM).

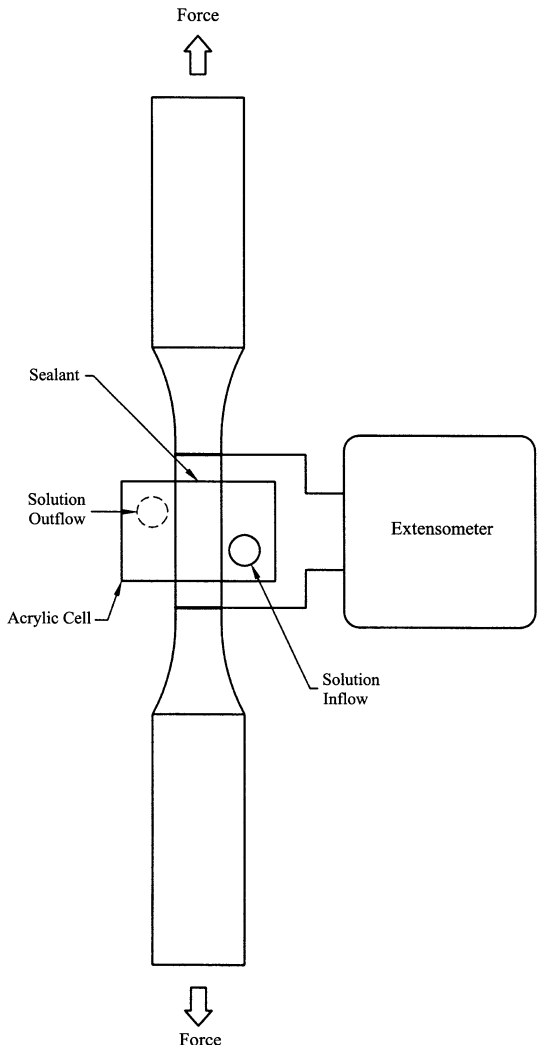

Fig. 1 Schematic view of the experimental set-up for axial LCCF test

Results and discussion

Effect of environment on low-cycle fatigue

A comparison of the experimental LCF results at 1 Hz in air and NaCl solution for each strain ratio is shown in Fig. 2 by plotting the strain amplitude versus number of cycles to failure on a log-log scale. In each strain ratio, all strain amplitudes could be divided into low strain amplitude region ($\varepsilon_a \leq 0.4\%$) and high strain amplitude region ($\varepsilon_a > 0.4\%$). It could be seen in Fig. 2 that at high strain amplitude region the differences in LCF life among the two given environments were smaller than those at low strain amplitude region for each strain ratio except $R = -1$. This implies that the environmental effects were not so clear at high strain amplitudes. Such a lack of environmental effect on the LCF might result from insufficient local dissolution of the given

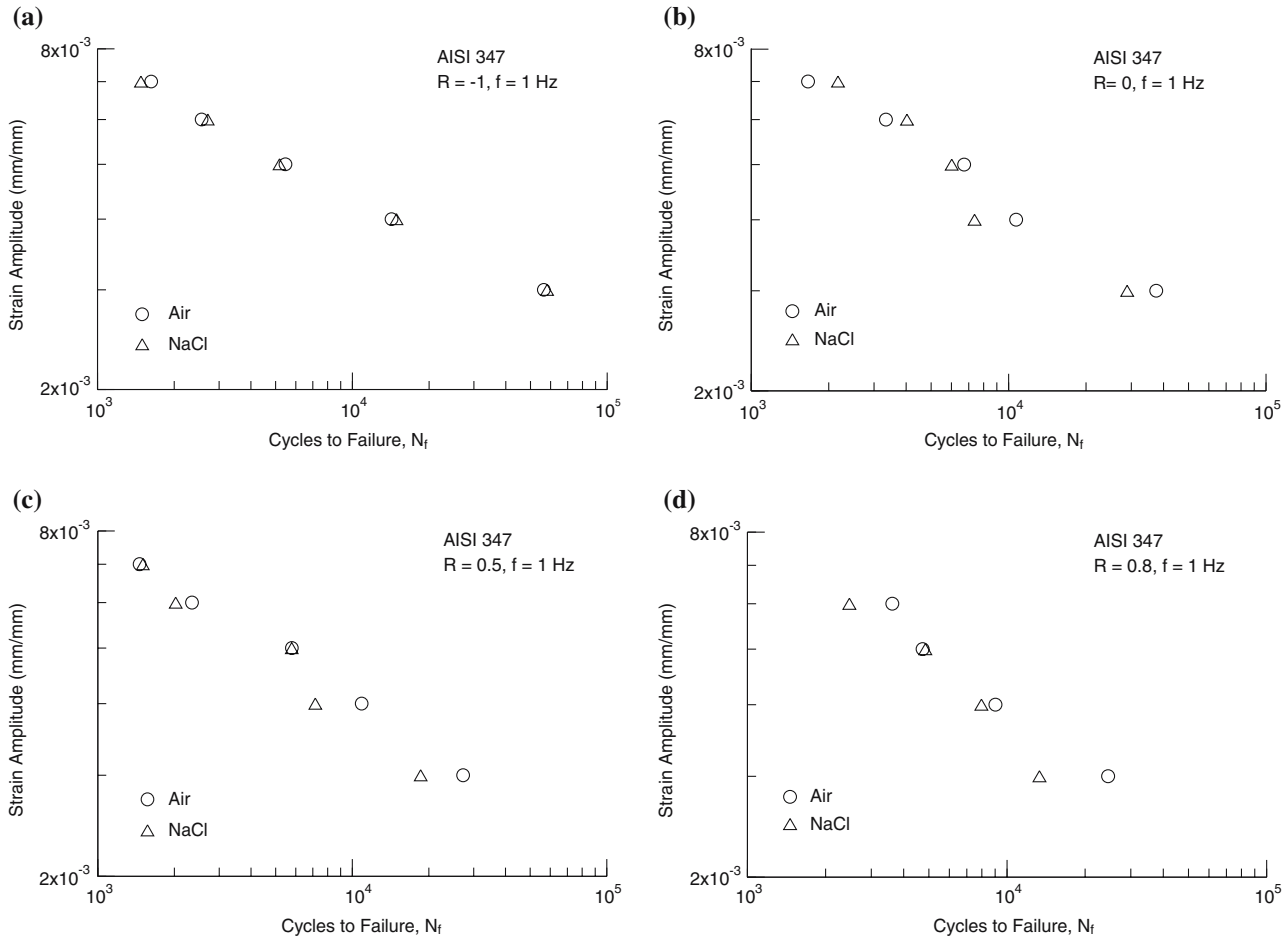

Fig. 2 Comparison of strain-life relationship in various environments for AISI 347 stainless steel at 1 Hz and various strain ratios: (**a**) R = -1, (**b**) R = 0, (**c**) R = 0.5, and (**d**) R = 0.8

alloy in NaCl solution. Magnin and Coudreuse [19] indicated that a crack in an aggressive environment could be initiated by a critical quantity of local dissolution of metal. In other words, a critical amount of local dissolution at slip bands should be reached before purely mechanical crack initiation occurred; otherwise the influence of corrosive solutions could be neglected. Therefore, it was suggested that the time interval during one loading cycle was not sufficient to complete dissolution of the freshly generated slip steps such that accelerated crack initiation did not occur in the salt water. In addition, even at higher strain ratios such as R = 0, 0.5, and 0.8, the mean stresses at high strain amplitudes were almost completely relaxed to zero, as shown in Table 1, such that no tensile-mean-stress enhanced corrosion would be expected in these conditions. In other words, the failure of specimen at this high strain amplitude region in the salt water was

Table 1 Mean stress at half life in LCF tests for AISI 347 stainless steel at various testing conditions

Total strain amplitude (%)	Mean stress in air (MPa)				Mean stress in NaCl (MPa)			
	R = –1	R = 0	R = 0.5	R = 0.8	R = –1	R = 0	R = 0.5	R = 0.8
0.3	6.41	8.21	10.16	16.56	1.78	3.78	11.76	20.01
0.4	–0.72	1.52	5.28	5.90	–2.53	0.86	4.96	9.73
0.5	0.01	1.40	0.25	3.46	–3.87	2.49	1.34	5.60
0.6	0.43	–1.15	0.19	1.03	–2.17	1.63	–0.05	4.30
0.7	–1.09	–0.30	–2.42	-	–0.17	–0.84	–0.72	-

still dominated by pure mechanical fatigue. Therefore, the LCCF lives were comparable with the fatigue lives in air.

At low strain amplitude region, it could be seen that at $R = -1$ the fatigue lives in both environments were comparable. However, at $R = 0$, 0.5 and 0.8, the fatigue lives in air were longer than those in NaCl solution. In other words, an environment-assisted, premature crack initiation did not occur at $R = -1$ but occurred at $R = 0$, 0.5 and 0.8 under a smaller strain amplitude. In addition, the degree of influence of such an environmental effect was generally increased with an increase in strain ratio, as shown in Fig. 2. Such dependence of environmental effect on strain ratio might be related to the difference in tensile mean stress.

Table 1 shows values of tensile mean stress at half-life with various strain amplitudes and ratios. It could be seen that the mean stress at low strain amplitude region was increased with increasing strain ratio in both given environments. It is well known that a tensile mean stress would generate irreversible slip steps, and then geometrical discontinuities could be formed at the roots of these slip steps. These geometrical discontinuities may act as both stress concentrators and regions where localized, concentrated environments can be formed. In salt water, hydrolysis of the corrosion product, chloride, generated an acidic solution that produced an active corroding anode at these geometrical discontinuities. Furthermore, in order to keep the electrical neutrality at these geometrical discontinuities, the chloride ions at the outer bulk environment would migrate into these areas leading to an environment of high chloride concentration. An enhanced corrosive effect would be expected for such areas with localized, high concentration of H^+ and Cl^- ions which both would enhance dissolution of metal [20]. The corrosion rate in these regions would be enhanced to dissolve the fresh slip steps generated in next loading cycle at these area. Therefore, crack initiation would be accelerated by such a localized acidification in NaCl solution such that the environmental effect would be more pronounced for a low strain amplitude at a greater strain ratio accompanied with a larger tensile mean stress.

A typical process of crack initiation under corrosion fatigue in salt solution involved evolution of a corrosion pit to become a crack. As a corrosion pit reached a critical size, a fissure would be formed at pit base and then grow to become a crack [21]. Such sharp fissures were indeed found in the current study for the specimens tested in salt water, as shown in Fig. 3. It could be seen in Fig. 3(b) that a sharp fissure was produced at a pit base leading to initiation of a crack from this fissure. The sharp fissures formed in NaCl solution would serve as effective stress concentrators and result in earlier crack initiation. Therefore, the LCF lives at low strain amplitudes in salt solution were shorter than those in air at higher strain ratios.

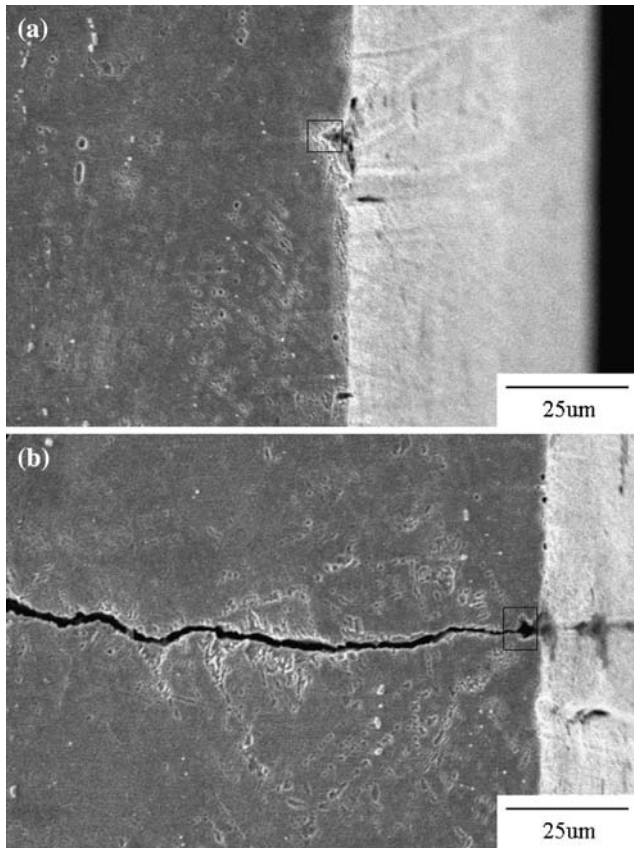

Fig. 3 SEM micrographs showing pitting morphology in an axially-sectioned specimen tested at $R = 0.5$ with a strain amplitude of 0.5% in 3.5% NaCl solution: (**a**) a pit on surface and (**b**) a crack developed from a pit

Effect of strain ratio on low-cycle corrosion fatigue

Comparisons of the LCF testing results at various strain ratios for each given environment are shown in Fig. 4. It could be seen that at low strain amplitude region the rank of fatigue life in both given environments generally took the following order: $R = -1 > R = 0 > R = 0.5 > R = 0.8$. These results could be attributed to a mean stress effect. In general, when specimens were subjected to a tensile mean stress, the crack initiation life would be shortened by accelerated extension of defects [22]. As indicated in Table 1, at low strain amplitude region the mean stress level at half life was increased with an increase in strain ratio. Therefore, at low strain amplitudes the reduced fatigue lives at higher strain ratios indeed resulted from higher tensile mean stresses.

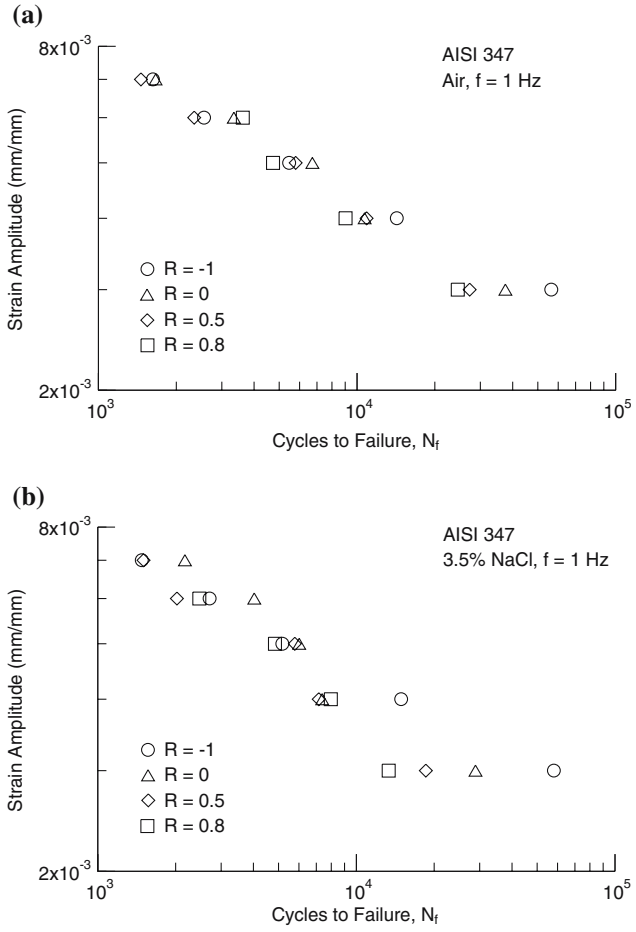

Fig. 4 Strain-life relationship at various strain ratios for AISI 347 stainless steel in different environments: (**a**) air and (**b**) 3.5% NaCl

In the corrosive environment, however, the reduced fatigue lives could also be partially attributed to the interaction between tensile mean stress and corrosive reaction. As mentioned above, a concentrated environment would be formed at the geometrical discontinuities which were generated by the irreversible slip steps due to a tensile mean stress. The corrosion rate was enhanced by the concentrated environment to corrode the fresh surface produced in next loading cycle. It was inferred that the corrosion rate would be enhanced when the tensile mean stress was increased. Therefore, it was suggested that the corrosive effect of the concentrated environments formed at the geometrical discontinuities might be enhanced with increasing strain ratio.

As shown in Fig. 4, the fatigue lives at various strain ratios were of no significant difference at high strain amplitudes in each given environment. It was suggested that these results might result from a complete relaxation of mean stress. As indicated in Table 1, the mean stress values at half life for high strain amplitudes were comparable and approximately equal to zero among the given strain ratios. Therefore, the fatigue lives at a high strain amplitude for various strain ratios were comparable in the current study. In addition, no additional environmental effect from the increase of strain ratio could be observed at high strain amplitudes due to the complete relaxation of tensile mean stress. At corrosive environments, the concentrated environment would be removed by the reverse slip steps as no tensile mean stress existed. The mechanism of enhanced corrosion rate was not available at this condition so the fatigue life at a large strain amplitude was also independent of strain ratio at a given aqueous solution.

Effects of frequency and waveform on low-cycle corrosion fatigue

Table 2 shows the fatigue life ratios in the given environments at a strain amplitude of 0.3% and strain ratio of 0.5 under various frequencies and waveforms. Note the life ratio hereby is defined as the number of cycles to failure in salt water divided by the corresponding one in air. It can be seen that the fatigue life ratio at 0.1 Hz in the aqueous solution was greater than the corresponding one at 1 Hz under a similar triangular loading waveform. The less corrosive effect at 0.1 Hz might be related to a lower corrosion rate resulting from a low strain rate. Maginin and Coudreuse [19] indicated that the corrosion rate was dependent on strain rate. At a low strain rate, more time was available to repair the slowly ruptured passive film and reduce the amount of unprotected fresh surface leading to a low corrosion rate. Therefore, a decrease in the amount of local dissolution during one loading cycle was expected for a low strain rate. Such a strain-rate effect might occur in the given alloy-aqueous environment system such that the fatigue life ratio at 0.1 Hz in NaCl was greater than that at 1 Hz.

As indicated in Table 2, fatigue life ratio in NaCl solution with a 10-s hold time at tensile peak strain was comparable with that at 1 Hz (0.71 vs. 0.68). Note that

Table 2 Fatigue life ratio for AISI 347 stainless steel at $R = 0.5$ with a strain amplitude of 0.3 % under various frequencies and waveforms in various environments

Environment	Fatigue life ratio (N/N_{air})		
	1 Hz	0.1 Hz	10-s hold time
Air	1	1	1
NaCl	0.68	0.87	0.71

the 10 s hold time was added at the tensile peak strain in a 1-Hz triangular loading waveform. In a study by Pyle et al. [23], a decay of transient current was observed within a hold period at peak strain under an applied passive potential for an 18/8 stainless steel in an acidic solution. A higher transient current indicated a greater corrosion rate. That result [23] implied that the ruptured passive film generated by plastic deformation could be partially repaired at this hold period to form new passive film. Similarly in the current study, repassivation might take place during the 10-s hold time to gradually reduce the corrosion rate in the given salt water. The fatigue life ratio in salt water with a 10-s hold time was comparable with that at 1 Hz implying that the amount of local dissolution per loading cycle for AISI 347 stainless steel in salt water was comparable under both loading conditions. In other words, no further significant dissolution of AISI 347 stainless steel took place during the hold period. Therefore, in salt water an additional hold period of 10 s at tensile peak strain did not generate more corrosive damages to accelerate crack initiation compared to the 1-Hz triangular loading waveform.

Low-cycle fatigue life prediction models

A total strain-life equation based on the plastic strain-life relation proposed by Coffin and Manson [24,25] was often used to correlate the fatigue life with reversed cyclic strain:

$$\frac{\Delta\varepsilon}{2} = \frac{\Delta\varepsilon_e}{2} + \frac{\Delta\varepsilon_p}{2} = \left(\frac{\sigma_f'}{E}\right)(2N_f)^b + \varepsilon_f'(2N_f)^c \quad (1)$$

where $\frac{\Delta\varepsilon}{2} = \varepsilon_a$ is the total strain amplitude, $\frac{\Delta\varepsilon_e}{2}$ is the elastic strain amplitude, $\frac{\Delta\varepsilon_p}{2}$ is the plastic strain amplitude, σ_f' is the fatigue strength coefficient, E is the elastic modulus, N_f is the number of cycles to failure, b is the fatigue strength exponent, ε_f' is the fatigue ductility coefficient, and c is the fatigue ductility exponent.

The σ_f', ε_f', b, and c are fatigue properties of material which can be obtained by separating the strain-life results of reversed cyclic strain tests ($R = -1$) into elastic and plastic portions, followed by curve fitting the elastic and plastic parts, respectively, according to Eq. (1).

Eq. (1) was then applied to correlate the strain amplitude with reversals to failure for the given environments, as shown in Fig. 5. The LCF parameters (σ_f', ε_f', b, c) in Eq. (1) were obtained from the fitted curves and listed in Table 3 for each environment. It could be seen in Fig. 5 that the Coffin-Manson relation

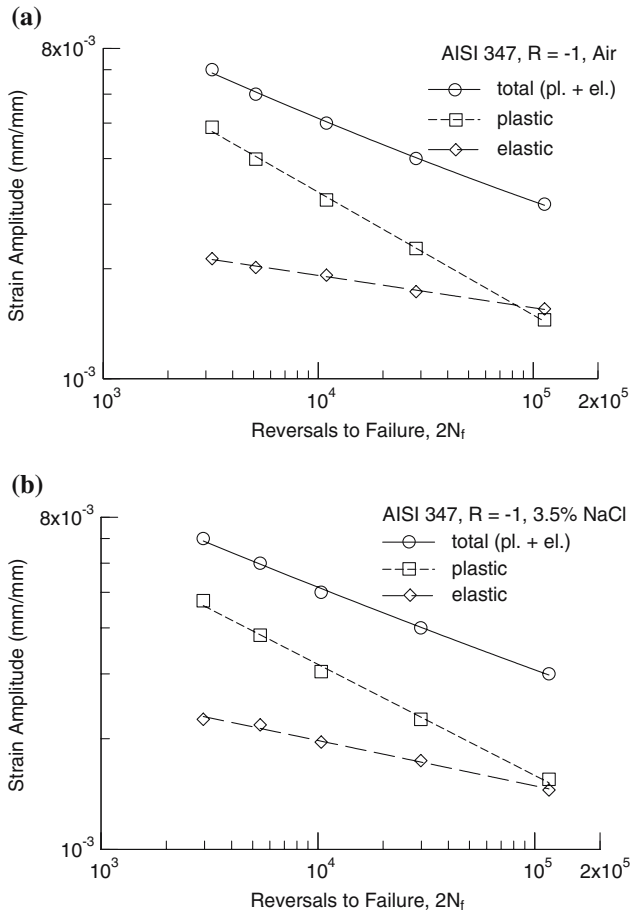

Fig. 5 Strain-life relationship at $R = -1$ for AISI 347 stainless steel in different environments: (**a**) air and (**b**) 3.5% NaCl

of Eq. (1) is an excellent fit to the two sets of experimental data. It could also be found that at total applied strain amplitudes of 0.4% to 0.7% the plastic portion is significantly greater than the elastic part in all given environments. This indicated that LCF in this high strain amplitude region was dominated by plastic deformation.

In order to estimate a fatigue damage event where mean stress is involved, the life prediction models are usually developed to consider mean stress effects on fatigue behavior. For example, Manson-Halford (MH) [26] and Smith-Watson-Topper (SWT) [27] proposed

Table 3 Values of parameters related to LCF properties of AISI 347 stainless steel in different environments

Environment	Fatigue strength exponent, b	Fatigue strength coefficient, σ_f' (MPa)	Fatigue ductility exponent, c	Fatigue ductility coefficient, ε_f'
Air	–0.088	821	–0.336	0.071
NaCl	–0.123	1,169	–0.302	0.051

some popular models to predict the fatigue behavior with mean stress. The MH [26] approach is given as follows:

$$\frac{\Delta\varepsilon}{2} = (\frac{\sigma'_f}{E})(2N^*)^b + \varepsilon'_f(2N^*)^c \quad (2)$$

where $N^* = N_f(1 - \frac{\sigma_m}{\sigma'_f})$ and σ_m is the mean stress. The SWT [27] model is expressed by the following equation:

$$\frac{\Delta\varepsilon}{2}\sigma_{max}E = (\sigma'_f)^2(2N_f)^{2b} + \sigma'_f\varepsilon'_fE(2N_f)^{b+c} \quad (3)$$

where σ_{max} is the maximum stress.

Here, the MH (Eq. (2)) and SWT (Eq. (3)) approaches were first used to estimate fatigue life for the given alloy at various strain ratios in different environments. Note that in the current study σ_m and σ_{max} were determined from the cyclic stress-strain curve at half life in each test. The values of constants σ_f', ε_f', b, and c in Table 3 were applied to generate the prediction results. For the M-H model, there is a good agreement between the experimental and predicted LCF lifetimes for air, while the predictions seem to slightly overestimate the fatigue lifetimes at low strain amplitude region for NaCl solution. However, the SWT model generally overestimated the fatigue lifetimes for both given environments. In this regard, neither approach can well predict the mean stress effects on the LCF life for the given alloy-environment systems. Therefore, modifications of these two approaches were proposed in the current study to seek a better prediction model for the LCF life of the given 347 stainless steel and environments.

A modified MH approach was proposed to correlate the strain amplitude (ε_a) with modified number of cycles to failure (N^*) by a simple power law, i.e., $\varepsilon_a \propto (N^*)^m$. In a similar way, a modified SWT approach was proposed to correlate the SWT parameter with fatigue life by a simple power law, i.e., $(\sigma_{max}\varepsilon_a) \propto (N_f)^n$. These modified relationships could be obtained by fitting the experimental data using a simple power law with linear regression analysis for each given environment, as shown in Figs. 6 and 7. The fitted power law relationships $\varepsilon_a \propto (N^*)^m$ and $(\sigma_{max}\varepsilon_a) \propto (N_f)^n$ for the given two environments were represented by the solid lines shown in Figs. 6 and 7, respectively. The obtained simple power law equation and correlation coefficient for both modified models in each environment were shown in Tables 4 and 5. Note the units for ε_a and σ_{max} in Tables 4 and 5 are mm/mm and MPa, respectively. The very high values of correlation coefficient shown in Tables 4 and 5 indicate that both modified approaches did an excellent job in estimating the LCF life with mean stress effects for the given alloy-environment systems. The correlation coefficient values for modified SWT approach were slightly greater than those for modified M-H approach. Furthermore, at low strain amplitude region the modified SWT approach showed less scattering in the lifetime data. Therefore, the modified SWT approach has the best ability among the several proposed approaches to predict the LCF life with a mean stress for the given testing conditions.

Fractography analysis

Fatigue fracture surface morphology near the crack initiation site for specimens tested at 1 Hz with low strain amplitudes in the given environments was exemplified in Figs. 8 and 9. The crack initiation sites

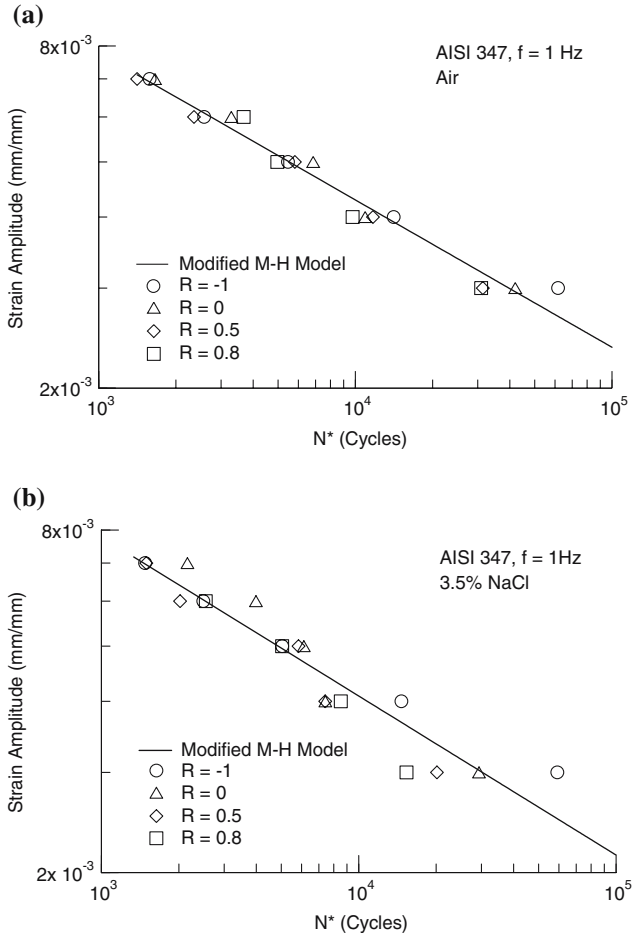

Fig. 6 Modified Manson and Halford relation for the LCF results of AISI 347 stainless steel in different environments: (**a**) air and (**b**) 3.5% NaCl

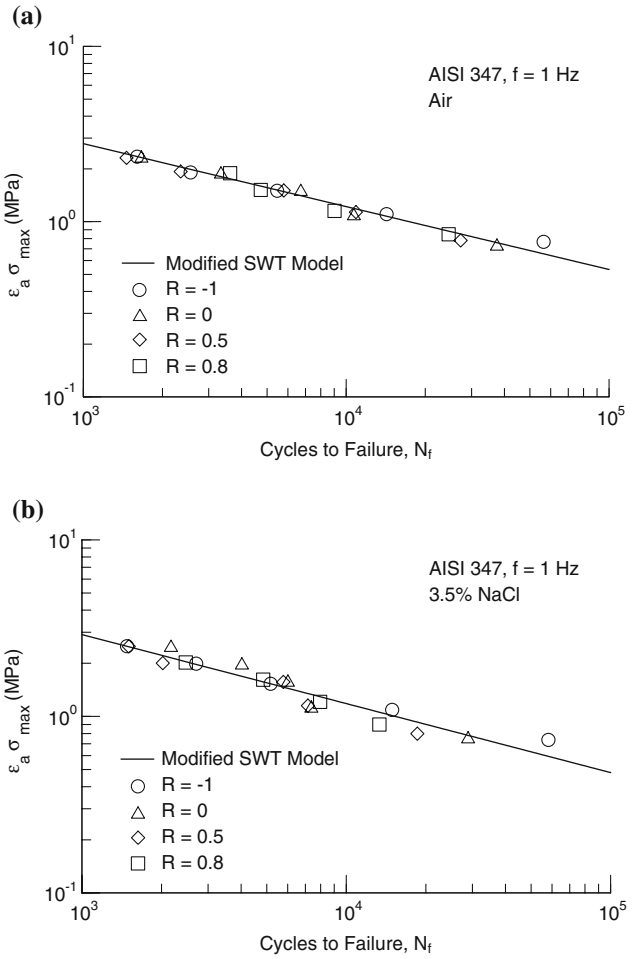

Fig. 7 Modified SWT relation for the LCF results of AISI 347 stainless steel in different environments: (**a**) air and (**b**) 3.5% NaCl

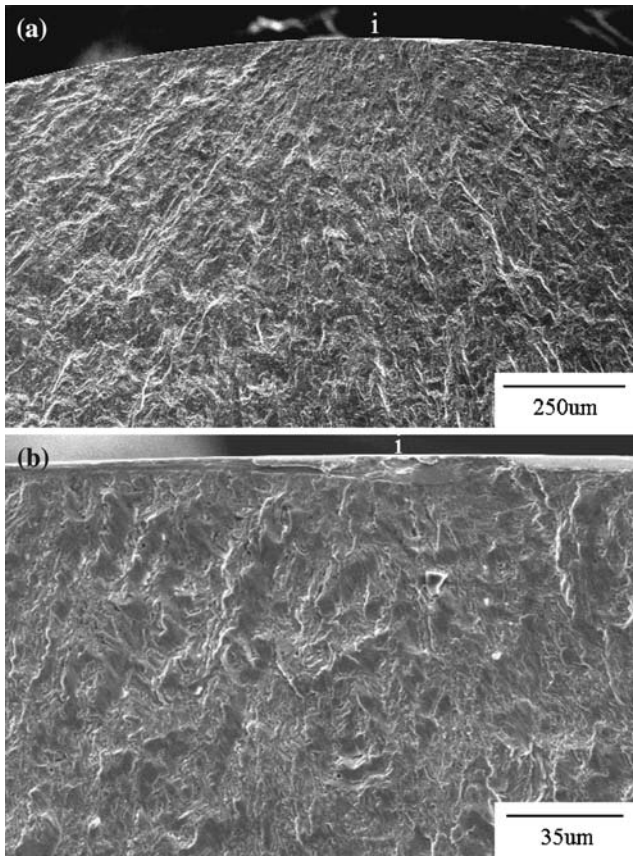

Fig. 8 SEM fractography of AISI 347 stainless steel tested at $R = 0$ with a strain amplitude of 0.3% and 1 Hz in air: (**a**) slow crack growth region and (**b**) fracture origin. (i: crack initiation site)

Table 4 The fitted simple power law relationship and correlation coefficient of a modified Manson-Halford approach in various environments

Environment	Fitted equation	Correlation coefficient (r^2)
Air	$\varepsilon_a = 0.047(N^*)^{-0.26}$	0.97
NaCl	$\varepsilon_a = 0.054(N^*)^{-0.28}$	0.90

Table 5 The fitted simple power law relationship and correlation coefficient of a modified SWT approach in various environments

Environment	Fitted equation	Correlation coefficient (r^2)
Air	$\varepsilon_a\sigma_{max} = 33.21(N_f)^{-0.36}$	0.97
NaCl	$\varepsilon_a\sigma_{max} = 43.26(N_f)^{-0.39}$	0.92

in these micrographs could be clearly identified for the given conditions. However, it could be found that fracture of specimen tested in the aqueous solution at a low strain amplitude originated from a corrosion-induced surface defect which was absent in the specimens tested in air. In salt water, the fresh surface generated by plastic deformation would be locally corroded by chloride ions to form pits serving as a stress concentrator to accelerate crack initiation. This is evidenced by the corrosion pit shown in Fig. 9(b). Similar fracture surface morphology can also be seen for the specimens tested at 0.1 Hz and 10-s hold time at tensile peak strain in NaCl under a low strain amplitude, as exemplified in Fig. 10. However, at high strain amplitude region, the crack initiation sites in the given aqueous solution could not be clearly identified in association with any corrosion-induced surface defect. It was inferred that LCCF fracture in the salt water at high strain amplitude region was indeed dominated by large plastic deformation caused by mechanical loading.

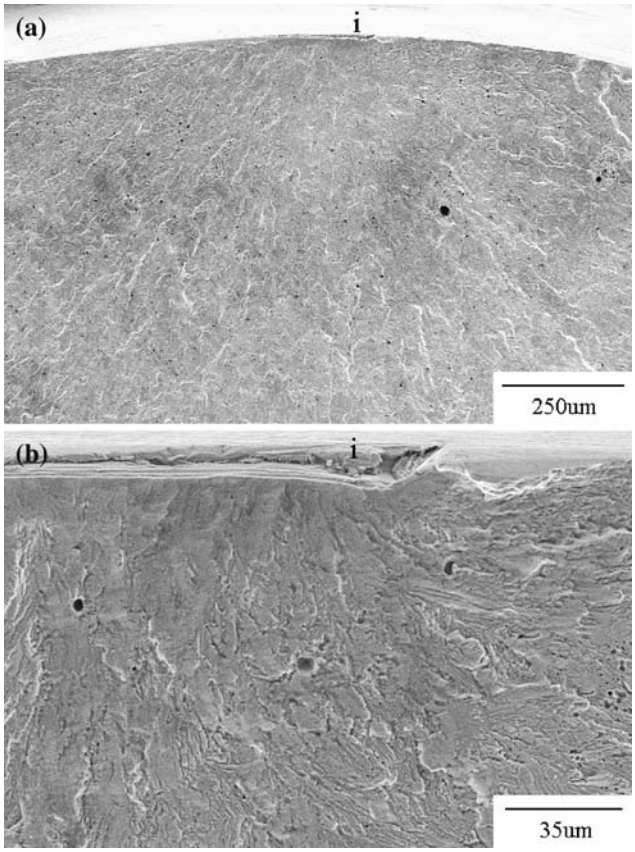

Fig. 9 SEM fractography of AISI 347 stainless steel tested at $R = 0$ with a strain amplitude of 0.3% and 1 Hz in 3.5% NaCl: (**a**) slow crack growth region and (**b**) fracture origin. (i: crack initiation site)

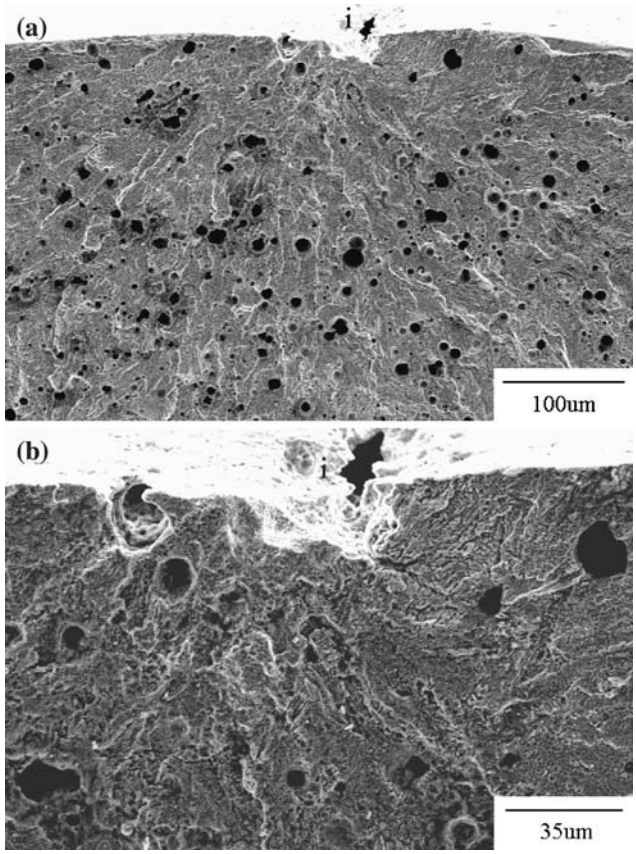

Fig. 10 SEM fractography of AISI 347 stainless steel tested at $R = 0.5$ with a strain amplitude of 0.3% and 0.1 Hz in 3.5% NaCl: (**a**) slow crack growth region and (**b**) fracture origin. (i: crack initiation site)

Conclusions

(1) For LCF behavior of AISI 347 stainless steel in NaCl solution, detrimental, environmental effects were only observed at low strain amplitude region. At high strain amplitude region, there was a lack of tensile-mean-stress enhanced corrosion and insufficient time for local dissolution such that no premature crack initiation was found.

(2) The corrosive effects of the given salt water on the LCF behavior at low strain amplitudes were enhanced with increasing strain ratio. This might be explained by an enhanced corrosive effect of a concentrated environment on the geometrical discontinuities generated by tensile mean stresses.

(3) A less corrosive effect was found in NaCl solution when the loading frequency was reduced from 1 to 0.1 Hz, presumably, resulting from a low localized corrosion rate under a low strain rate. An additional hold period of 10 s at tensile peak strain in salt water did not generate more corrosive damages to accelerate crack initiation compared to a 1-Hz triangular loading waveform.

(4) At high strain amplitude region, the fatigue fracture in NaCl solution was dominated by large plastic deformation, while at low strain amplitude region the fatigue fracture originated from corrosion-induced surface defects.

(5) A modified SWT approach and a modified Manson-Halford approach were proposed and did an excellent work in correlating the LCF lifetime with mean stress for the given testing conditions.

Acknowledgements This work was supported by the National Science Council and Atomic Energy Council of the Republic of China (Taiwan) under Contract Nos. NSC-90-2623-7-008-006-NU and NSC 91-2623-7-008-001-NU.

References

1. Smith WF (1993) Structure and Properties of Engineering Alloys, 2nd Ed. McGraw Hill, Inc., New York, p 317
2. Ben-Haroe I, Rosen A, Hall IW (1993) Mater Sci Tech 9:620

3. Ayer R, Klein CF, Marzinsky CN (1992) Metall Trans A 23:2455
4. Hickling J, Wieling N (1981) Corrosion 37:147
5. Schweinsberg DP, Sun B, Otieno-Alego V (1994) J Appl Electrochem 24:803
6. Schweinsberg DP, Sun B, Cheng M, Flitt H (1993) J Appl Electrochem 23:1097
7. Schweinsberg DP, Sun B, Cheng M, Flitt H (1994) Corrosion Sci 36:361
8. Tyson W (1984) Metall Trans A 15:1475
9. Rozenak P, Eliezer D (1983) Mater Sci Eng 61:31
10. Rozenak P, Eliezer D (1989) Metall Trans A 20:2187
11. Rozenak P (1990) J Mater Sci 25:2532
12. Gladwin DN, Priest RH, Miller DA (1989) Mater Sci Tech 5:40
13. Senior BA (1990) Mater Sci Eng A130:51
14. Senior BA, Maguire J, Evans CA (1991) Mater Sci Eng A138:103
15. Ortner SR, Hippsley CA (1992) Mater Sci Tech 8:883
16. Ortner SR, Hippsley CA (1995) Mater Sci Tech 11:998
17. Asm International Handbook Committee (1990) In: Metals Handbook, 10th Ed., vol 1, Properties and Selection: Irons, Steels, and High-Performance Alloys. ASM International, Materials Park, OH, USA, p 870
18. Lin C-K, Lan I-L (2004) J Mater Sci 39:6901
19. Magnin T, Coudreuse L (1985) Mater Sci Eng 72:125
20. Jones DA (1996) Principles and Prevention of Corrosion, 2nd Ed. Prentice Hall, Upper Saddle River, NJ, USA, p 209
21. Bayoumi MR (1993) Eng Fract Mech 45:297
22. Fang D, Berkovits A (1994) Inter J Fatigue 16:429
23. Pyle T, Rollins V, Howard D (1975) J Electrochem Soc 122:1445
24. Coffin LF (1954) Trans ASME 76:931
25. Mason SS (1953) Heat Transfer Symposium. University of Michigan Engineering Research Institute, Ann Arbor, MI, USA, p 9
26. Manson SS, Halford GR (1981) Inter J Fract 17:169 and R35
27. Smith KN, Watson P, Topper TH (1970) J Mater 5:767